SB³C2023
Summer Biomechanics, Bioengineering and Biotransport Conference
June 4-8, Vail, CO, USA

END-TO-END 3D GEOMETRIC MODEL RECONSTRUCTION OF PELVIC ORGANS BASED ON 3D MAGNETIC RESONANCE IMAGING AND DEEP LEARNING

Hui Wang (1), Xiaowei Li (2), Chenxin Zhang (1), Xiuli Sun (2), Jianliu Wang (2), Jiajia Luo (1)

(1) Biomedical Engineering Department, Peking University, Beijing, China
(2) Department of Obstetrics and Gynecology, Peking University People's Hospital, Beijing, China

INTRODUCTION

Reconstruction of 3D geometric models of pelvic organs based on 3D magnetic resonance imaging (MRI) is a very important and challenging task for computer-aided diagnosis, treatment and prognosis of female pelvic organ prolapse. The 3D geometric model can show the spatial structure of the organ, help the physician visualize the specific shape of the organ, analyze the etiology [1], and provide a good basis for subsequent finite element analysis [2] and surgical planning. Traditional methods usually first manually or automatically segment 2D MRI slices, and then perform post-processing such as 3D geometric model reconstruction and complex geometric repair based on the segmentation results. However, due to the complex shape of the pelvic organs, the traditional methods still have some problems, such as complex manual operations, high workload and long working time.

Deep learning has been widely used in computer vision tasks in the past decade, for automatic natural image classification, detection, and segmentation. There have also been some methods to automatically segment MRIs using deep learning. However, the segmentation results still require manual post-processing to make them conform to the real 3D geometry. In addition, the error tolerance rate of such automatic segmentation method is quite low. Once there is a segmentation error in one slice, the whole structure can be changed significantly, which affects the reconstruction of the 3D geometric model. End-to-end deep learning could directly learn the process "from MRI to the final 3D geometric model". This not only automates the reconstruction process, but also makes it possible to focus on the global structural information of the 3D geometric model, which in turn has a higher error tolerance rate and more realistic reconstruction results.

In this work, we aimed to develop an end-to-end deep learning-based reconstruction technique for 3D geometric model reconstruction of pelvic organs from 3D MRI.

METHODS

Figure 1 shows a proposed architecture for the end-to-end 3D geometric model reconstruction, along with exemplary inputs and outputs. For example, a set of 3D MRIs (where 480 × 480 is the size of one slice and 18 is the number of slices per set) and a spherical point cloud (uniformly sampled from a spherical 3D geometric model with diameter 1) were used as inputs to predict the 3D geometric model of

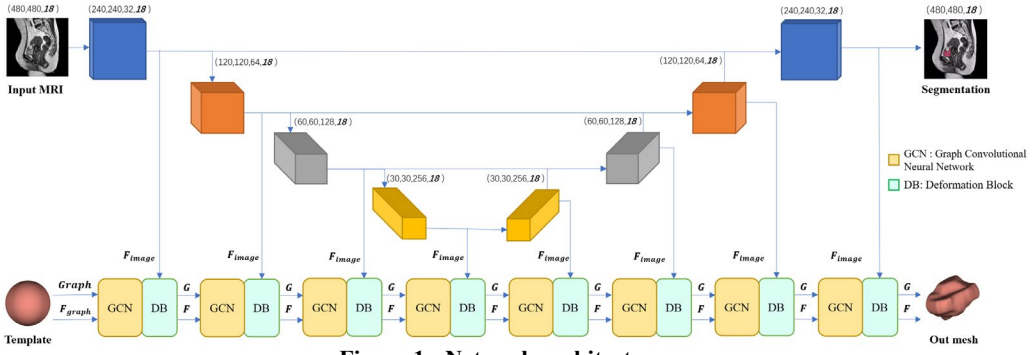

Figure 1: Network architecture.

the pelvic organs. First, a convolutional neural network (CNN) was used to extract layer-specific image features. Then, the spherical point cloud was constructed into a graph, and a graph convolutional neural network (GCN) was used to extract 3D structural features. GCN is a feature extractor for graph data structure, which has been widely used in 3D shape analysis in recent years. It can exchange features between neighboring nodes and eventually return to each node. In addition, a Deformation Block (DB) was designed to integrate image features with 3D structural features and transform spherical point cloud into a new point cloud. This completes a deformation of the point cloud. The above process was repeated eight times to extract deeper and more comprehensive feature information. Finally, the transformed point cloud was generated with the corresponding 3D geometric model of the organ. A manually reconstructed 3D geometric model was used as the ground-truth for the supervised training process.

The detailed structure of the Deformation Block (DB) is shown in Figure 2. A CNN was first used to encode the image information into a 1D vector. Next, each point of the sphere was concatenated with this 1D vector, and a multilayer perceptron (MLP) was used to learn the global features of the point cloud. We concatenate this feature with the 3D structural feature extracted by the GCN. Next, another MLP was used to learn the global changes, and EdgeConv [4] was used to learn the local changes to reconstruct the point cloud. Finally, the PointNet [5] was used to reconstruct the new point cloud.

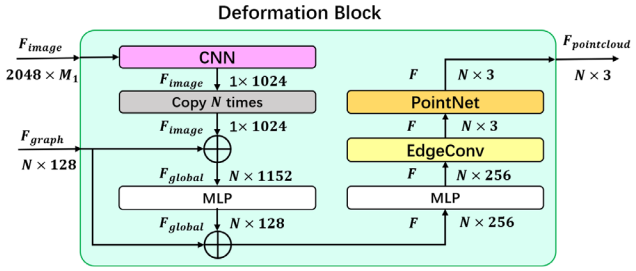

Figure 2: The detailed structure of the Deformation Block.

Several loss functions [6] were used to train our network, including Chamfer distance loss, Edge loss, and Laplacian loss, which were defined as follows.

$$L_{CD} = \sum_p min_g \|p - g\|_2^2 + \sum_g min_p \|p - g\|_2^2 \quad (1)$$

where p is the vertex coordinate of the predicted surface mesh, and g is the vertex coordinate of the ground-truth surface mesh.

$$L_{edge} = \sum_p \sum_{k \in N(p)} \|p - k\|_2^2 \quad (2)$$

where $N(p)$ are the neighbor vertices of p.

$$L_{Lap} = \sum_p \left\| \delta_p' - \delta_p \right\|_2^2, \delta_p = p - \sum_{k \in N(p)} \frac{k}{\|N(p)\|} \quad (3)$$

where δ_p and δ_p' are the Laplacian coordinates of vertex p before and after deformation.

The overall loss is a weighted sum of all four losses, defined as:

$$L = \lambda_1 L_{CD} + \lambda_2 L_{edge} + \lambda_3 L_{Lap} \quad (4)$$

where $\lambda_1 = 1.0, \lambda_2 = 0.01, \lambda_3 = 0.1$.

Chamfer distance (CD), Earth Mover's Distance (EMD), PC-to-PC L2 Distance (L2) and PC-to-PC L1 Distance (L1) were used as the evaluation metrics.

We used the Adam optimizer with a learning rate $1e^{-4}$ and a batch size of 2 for training in all experiments conducted. The network was implemented using Python 3.6.0, Pytorch 1.10.0, Dgl 0.7.2, and all experiments were streamlined and executed on an Nvidia Titan RTX graphic card with 24GB of computational memory.

We built a 3D MR dataset with 17 subjects from Peking University People's Hospital. Specifically, the T2 3D sagittal MR data of each subject at rest were used. The spacing of the MR images was 2 mm with a slice thickness of 2 mm. We randomly divided the annotated dataset into a training set (13 series) and a testing set (4 series). Each training sample contains a source-target pair, where the former is the original 3D MR image and the latter is the corresponding bladder surface mesh. To make the deformation process more reasonable, we first normalized each coordinate value of the real bladder to a range of 0 to 1. Then we moved the geometric center of the original sphere and the geometric center of the normalized real bladder to the origin (0,0,0). To prove the effectiveness of our model, we compared it with two other advanced 3D reconstruction of natural objects, including Pixel2mesh and Pixel2mesh++.

RESULTS

The testing result of the 3D reconstruction with comparison is summarized in Figure 3.

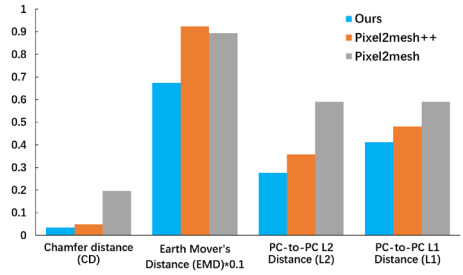

Figure 3: 3D reconstruction performance on the testing set. Smaller metrics better 3D reconstruction results.

In addition, the visualization results of the 3D reconstruction of the bladders of three subjects in the testing set are shown in Figure 4. From the results, our 3D reconstruction results are close to the ground-truth.

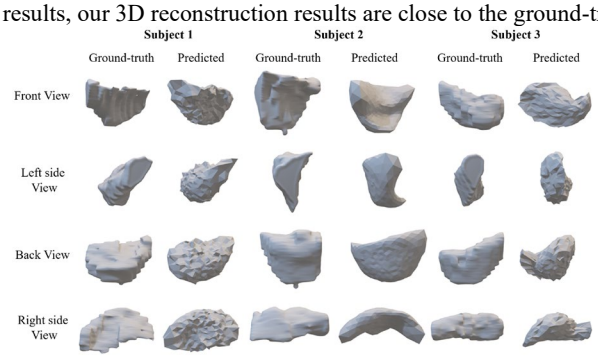

Figure 4: A visual comparison of 3D reconstruction results. Results of different views were compared with the ground truth labeling.

DISCUSSION

This study presents a novel end-to-end deep learning method with the CNN and GCN for fast reconstruction of 3D geometric models of pelvic organs from 3D MRI. Unlike traditional manual methods that are time-consuming and laborious, our method takes only 3 seconds. The experimental results demonstrate that the proposed network has achieved good qualitative and quantitative results in 3D reconstruction of the bladder. In the future, a larger training dataset will be expected to improve the reconstruction process.

ACKNOWLEDGEMENTS

NSFC Grant 31870942, Peking University Clinical Medicine Plus X-Young Scholars Project PKU2020LCXQ017 and PKU2021LCXQ028, PKU-Baidu Fund 2020BD039.

REFERENCES

[1] Luo et al., *Am J Obstet Gynecol*, 205(4), 2011.
[2] Luo et al., *J Biomech*, 48(9):1580-1586, 2015.
[3] Feng et al., *Med Phys*, 47(9):4281-4293, 2020.
[4] Wang et al., *Acm T Graphic*, 38(5), 2019.
[5] Charles et al., *CVPR 2017*, 77-81, 2017.
[6] Chen et al., *Med Image Anal 2021*, 74, 2021.